

- Phys. Chem.*, **93**, 6463 (1989).
11. M. K. Song, H. Chon, and M. S. Jhon, *J. Phys. Chem.*, **94**, 7671 (1990).
 12. M. K. Song, K. T. No, H. Chon, and M. S. Jhon, *J. Mol. Catal.*, **47**, 73 (1988).
 13. R. L. Yanagida, A. A. Amaro, and K. Seff, *J. Phys. Chem.*, **77**, 805 (1973).
 14. L. Verlet, *Phys. Rev.*, **159**, 98 (1968).
 15. D. L. Ermak and J. A. McCammon, *J. Chem. Phys.*, **69**, 1352 (1978).
 16. E. Dickinson, S. A. Allison, and J. A. McCammon, *J. Chem. Soc. Faraday Trans. 2*, **81**, 591 (1985).

Two Crystal Structures of Dehydrated Fully Ca²⁺-Exchanged Zeolite A Reacting with Rubidium Vapor

Seong Hwan Song and Yang Kim*

Department of Chemical Engineering, Dongseo University, Pusan 616-012

**Department of Chemistry, Pusan National University, Pusan 609-735*

Received October 20, 1992

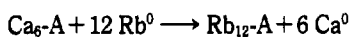
Two single crystals of fully dehydrated Rb⁺-exchanged zeolite A have been prepared by the reduction of all Ca²⁺ ions in dehydrated Ca₆-A by rubidium vapor. Their structures were determined by single crystal X-ray diffraction methods in the cubic space group *Pm3m* ($a=12.160(2)$ Å and $12.166(2)$ Å) at 22(1)°C. In these structures, 12.4(2) to 13.3(2) Rb species are found per unit cell, more than 12 Rb⁺ ions needed to balance the anionic charge of the zeolite framework, indicating that the sorption Rb⁰ has occurred. In each structure, three Rb⁺ ions per unit cell are located at the centers of the 8-rings. Six to eight Rb⁺ ions are found opposite the 6-rings on threefold axes, and three Rb⁺ ions are found in a sodalite unit. About 0.5 Rb⁺ ion lies opposite a 4-ring. The structural analysis indicates the presence of a triangular rubidium cluster in the sodalite cavities. The triangular rubidium clusters may be stabilized by the coordination to two and/or three rubidium ions in the large cavity. Therefore, this cluster may be viewed as (Rb₃)⁴⁺ and/or (Rb₆)⁴⁺.

Introduction

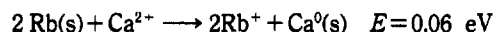
During the past decade, a series of attempts had failed to achieve the fully Rb⁺-exchanged zeolite A.^{1,2} Seff *et al.* reported that large monovalent Rb⁺ ions exchanged incompletely into zeolite A by flow methods.^{1,2} In dehydrated eleven-twelfths Rb⁺-exchanged zeolite A, three equivalent Rb⁺ ions lie at the center of the oxygen 8-rings, and five equivalent Rb⁺ ions lie on threefold axes opposite the 6-rings in the large cavity. The remaining three Rb⁺ ions are non-equivalent and lie on each different threefold axis of unit cell. One Na⁺ ion lies almost at the center of a 6-ring.¹

Recently, fully Cs⁺-exchanged zeolite A has been synthesized by the reduction of all of the Na⁺ ions in Na₁₂-A by cesium vapor.^{3,4} The redox reaction goes to completion at 250°C with 0.1 torr of Cs⁰ to give Cs₁₂-A·1/2Cs. In this structure, each extra Cs atom associates with two or three Cs⁺ ions to form linear (Cs₃)²⁺ or (Cs₄)³⁺ clusters. These clusters lie on threefold axes and extend through the centers of sodalite units.

This work was initiated with the hope that the intrazeolitic redox potential for the reaction



would be positive at the conditions employed to result in complete exchange. The *E* values, not involving the zeolite, are easily calculated.⁵



The resulting material may be of interest because the volume of the exchangeable cations would be large and some extra Rb⁰ atoms may be present, forming Rb clusters as were Cs⁰ atoms in the structure of the dehydrated Na₁₂-A reacted with cesium. These extra Rb atoms are likely to complex to Rb⁺ cations to form rubidium clusters.

Experimental

Single crystals of zeolite 4A were prepared by Charnell's methods⁶ using seed crystals from a previous synthesis. A single crystal about 0.085 mm on an edge was lodged in a fine glass capillary. To prepare Ca₆-A, an exchange solution of 0.04325 M Ca(NO₃)₂ (Aldrich, 99.997%) and 0.00675 M CaO (Aldrich, 99.995%) with a total concentration of 0.05 M was allowed to flow past each crystal at a velocity of approximately 1.0 cm/sec for 3 days at 21(1)°C. The crystals remained colorless.

The hydrated fully Ca²⁺-exchanged zeolite A was dehydrated at 360°C and 2×10⁻⁶ Torr for 2 days. Rubidium vapor was introduced by distillation from a side-arm break-seal ampoule to the glass-tube extension of the crystal-containing capillary. This glass reaction vessel was then sealed off under vacuum placed within a pair of cylindrical horizontal oven, axis colinear, attached. The oven about crystal was

always maintained at a higher temperature than that about the rubidium metal so that rubidium would not distill onto the crystal.

The first reaction, Rb(g) with Ca₆-A, was carried out at 250°C with *ca.* 0.1 Torr of Rb(g) (Rb(l) at 220°C)⁸ for 2 hrs. The second reaction was carried out at 250°C with *ca.* 0.1 Torr of Rb(g) (Rb(l) at 220°C) for 24 hrs. The resulting crystals were sealed off from their reaction vessels by torch after cooling to room temperature. Both crystals has become black in color.

Diffraction intensities were subsequently collected at 22(1) °C. The space group *Pm3m* (no systematic absences) was used throughout this work for reasons discussed previously.^{9,10} An Enraf-Nonius 4-circle computer-controlled CAD-4 diffractometer, equipped with scintillation counter, pulse-height analyzer, a PDP micro 11/73 computer, and graphite monochromator were used. Molybdenum radiation ($K\alpha_1$, $\lambda=0.70930$ Å; $K\alpha_2$, $\lambda=0.71359$ Å) was used for all experiments. In each case, the unit cell constant, 12.160(2) Å, and 12.166(2) Å for crystals 1 and 2, respectively, was determined by a least-squares treatment of 25 intense reflections for which $18^\circ < 2\theta < 25^\circ$. For each crystal, reflections from two intensity-equivalent regions of reciprocal space (hkl , $h \leq k \leq l$ and lkh , $l \leq h \leq k$) were examined. The intensities were measured using the $\omega-2\theta$ scan technique over a scan width of $(0.80 + 0.344 \tan\theta)$ in ω . The data were collected using variable scan speeds. Most reflections were observed at slow scan speeds, from 0.25 to 0.31 deg/min in ω . The intensities of three ref-

lections in diverse regions of reciprocal space were recorded every three hours to monitor crystal and instrument stability. Only small, random fluctuations of these check reflections were noted during the course of data collection.

For each region of reciprocal space, the intensities of all lattice points for which $2\theta < 70^\circ$ were recorded. The raw data from each region were corrected for Lorentz and polarization effects including that due to incident beam monochromatization; The reduced intensities were merged and the resultant estimated standard deviations were assigned to each average reflection by the computer programs, PAINT and WEIGHT.¹¹ Absorption corrections ($\mu R=0.38$ for both crystals) were judged to be negligible.¹² Of the 853 and 850 pairs of reflections of crystals 1 and 2, only the 111 and 61 pairs, respectively, for which $I > 3\sigma(I)$ were used in subsequent structure determinations.

Structure Determination

Crystal 1. Ca₆-A Treated with 0.1 Torr of Rb Vapor at 220°C for 2 hrs. Full-matrix least-squares refinement was initiated with the atomic parameters of the framework atoms [(Si, Al), O(1), O(2), and O(3)] of dehydrated Rb₁₁Na₁-A¹. Anisotropic refinement of the frameworks converged to an unweighted R_1 index, $[\sum(|F_o - |F_c||) / \sum F_o]$, of 0.420 and a weighted R_2 index, $(\sum w(F_o - |F_c|)^2 / \sum w F_o^2)^{1/2}$, of 0.530.

A subsequent Fourier synthesis revealed three large peaks at (0.0, 0.5, 0.5) of height 28.0(40) e⁻³, (0.27, 0.27, 0.27)

Table 1. ^aPositional, Thermal, and Occupancy Parameters

Crystal 1. Dehydrated Ca₆-A Treated with 0.1 Torr of Rb Vapor at 250°C for 2 hrs

Atom	Wyc. pos.	<i>x</i>	<i>y</i>	<i>z</i>	or b_{Biso}^{11}	β_{22}	β_{33}	β_{12}	β_{13}	β_{23}	Occupancy varied
(Si, Al)	24(<i>k</i>)	0	1846(5)	3723(5)	29(40)	62(5)	32(5)	0	0	20(10)	24 ^c
O(1)	12(<i>h</i>)	0	2260(20)	5000	180(30)	90(20)	20(20)	0	0	0	12
O(2)	12(<i>i</i>)	0	2910(10)	2910(10)	130(20)	50(10)	50(10)	0	0	60(40)	12
O(3)	24(<i>m</i>)	1124(8)	1124(8)	3410(10)	110(10)	110(10)	100(20)	60(30)	80(20)	80(20)	24
Rb(1)	3(<i>c</i>)	0	5000	5000	130(10)	182(8)	182(8)	0	0	0	3.0
Rb(2)	8(<i>g</i>)	2718(4)	2718(4)	2718(4)	119(3)	119(3)	119(3)	71(9)	71(9)	71(9)	6.01(5)
Rb(3)	8(<i>g</i>)	1070(10)	1070(10)	1070(10)	300(10)	300(10)	300(10)	220(30)	220(30)	220(30)	2.96(8)
Rb(4)	12(<i>j</i>)	2590(200)	2590(200)	5000	10(Fixed)						0.18(8)

Crystal 2. Dehydrated Ca₆-A Treated with 0.1 Torr of Rb Vapor at 250°C for 24 hrs

Atom	Wyc. pos.	<i>x</i>	<i>y</i>	<i>z</i>	or b_{Biso}^{11}	β_{22}	β_{33}	β_{12}	β_{13}	β_{23}	Occupancy varied
(Si, Al)	24(<i>k</i>)	0	1840(10)	3730(1)	40(10)	70(10)	30(10)	0	0	40(30)	24 ^c
O(1)	12(<i>h</i>)	0	2210(40)	5000	80(50)	160(60)	20(30)	0	0	0	12
O(2)	12(<i>i</i>)	0	2830(30)	2830(30)	150(50)	100(40)	100(40)	0	0	100(100)	12
O(3)	24(<i>m</i>)	1160(20)	1160(20)	3450(30)	140(20)	140(20)	100(30)	220(70)	120(60)	120(60)	24
Rb(1)	3(<i>c</i>)	0	5000	5000	140(30)	160(20)	160(20)	0	0	0	3.0
Rb(2)	8(<i>g</i>)	2727(7)	2727(7)	2727(7)	142(7)	142(7)	142(7)	70(20)	70(20)	70(20)	6.78(12)
Rb(3)	8(<i>g</i>)	1090(20)	1090(20)	1090(20)	120(10)	120(10)	120(10)	70(40)	70(40)	70(40)	2.92(10)
Rb(4)	12(<i>j</i>)	2670(100)	2670(100)	5000	10(Fixed)						0.68(16)

^aPositional and anisotropic thermal parameters are given $\times 10^4$. Numbers in parentheses are the esd's in the units of the least significant digit given for the corresponding parameter. ^bThe anisotropic temperature factor = $\exp[-(\beta_{11}h^2 + \beta_{22}k^2 + \beta_{33}l^2 + \beta_{12}hk + \beta_{13}hl + \beta_{23}kl)]$. ^cOccupancy factors are given as the number of atoms or ions per unit cell. Occupancy for (Si)=12; occupancy for (Al)=12.

of height $42(2) \text{ e}\text{\AA}^{-3}$, and $(0.134, 0.134, 0.134)$ of height $19.7(2) \text{ e}\text{\AA}^{-3}$. Anisotropic refinement of the framework atoms and the Rb^+ ions at Rb(1), Rb(2), and Rb(3) converged to $R_1 = 0.072$ and $R_2 = 0.065$ with occupancies 3.0, 6.01, and 2.96, respectively (see Table 1). A subsequent difference Fourier synthesis revealed a peak at $(0.26, 0.26, 0.5)$ of height $2.5(4) \text{ e}\text{\AA}^{-3}$. This peak was refined but with an usually large thermal parameter. Therefore, the isotropic thermal parameter of Rb(4) was fixed at the more reasonable value given in Table 1. Allowing all Rb(i) $i=1-4$ occupancies to vary except that at Rb(1), which was not permitted to exceed 3.0 (its maximum occupancy by symmetry), and allowing all anisotropic thermal parameters to vary except for that Rb(4), led to $R_1 = 0.067$ and $R_2 = 0.054$ (Table 1) (for comparison, trial least-squares refinements using 247 independent reflections for which $I > 1\sigma(I)$ converged to $R_1 = 0.207$ and $R_2 = 0.081$). However, the positional, thermal, and occupancy parameters were refined to almost the same values of crystal 1 of Table 1). A final difference Fourier synthesis was featureless except for one insignificant peak at the center of the large cavity $(0.5, 0.5, 0.5)$; peak height = $1.9(6) \text{ e}\text{\AA}^{-3}$.

Crystal 2. $\text{Ca}_6\text{-A}$ Treated with 0.1 Torr of Rb Vapor at 220°C for 24 hrs. Full-matrix least-squares refinement was initiated using the parameters of all framework atoms and Rb^+ ions in crystal 1 except Rb(4). Simultaneous positional, occupancy, and anisotropic thermal parameter refinement converged to $R_1 = 0.079$ and $R_2 = 0.057$. Refinement including Rb(4), which appeared on a subsequent difference Fourier function at $(0.26, 0.26, 0.5)$ with a peak of height $3.2(3) \text{ e}\text{\AA}^{-3}$, lowered R_1 to 0.074 and R_2 to 0.051. The final difference function was featureless except for a peak at $(0.5, 0.5, 0.5)$; peak height = $2.3(4) \text{ e}\text{\AA}^{-3}$ as crystal 1.

All shifts in the final cycles of least-squares refinement for both crystals were less than 0.1% of their corresponding standard deviations.

For all structures, the full-matrix least-squares program used minimized $\sum w(F_o - |F_c|)^2$; the weight w of an observation was the reciprocal square of $\sigma(F)$, its standard deviation. Atomic scattering factors for Rb^+ , O^- , and $(\text{Si}, \text{Al})^{1.75+}$ were used.^{13,14} The function describing $(\text{Si}, \text{Al})^{1.75+}$ is the mean of the Si^0 , Si^{4+} , Al^0 , and Al^{3+} function. All scattering factors were modified to account for the anomalous dispersion correction.^{15,16} The final structural parameters and selected interatomic distances and angles are presented in Tables 1 and 2, respectively.

Discussion

In both crystal structures, Rb^+ ions are distributed over four crystallographic sites, as summarized in Table 1. These structures differ only in the occupancies at Rb(2) and Rb(4).

In each structure, three Rb^+ ions at Rb(1) fill the equi-points of symmetry C_{4h} (D_{4h} in $Pm\bar{3}m$) at the center of the 8-rings (see Figures 1 and 2), as they have in all previously reported Rb^+ -exchanged zeolite A.¹⁷⁻¹⁹ Each Rb(1) cation is *ca.* $3.75(5) \text{ \AA}$ from four O(1) oxygens and *ca.* $3.53(3) \text{ \AA}$ from four O(2)'s (see interatomic distances in Table 2). These distances are substantially longer than the sum of the ionic radii of O^{2-} and Rb^+ , 2.79 \AA .²⁰

In the large cavity, Rb(2) is *ca.* $2.85(2) \text{ \AA}$ from the three O(3) oxygens of its 6-ring and *ca.* $1.72(1) \text{ \AA}$ from the (111)

Table 2. Selected Interatomic Distances (\AA) and Angles (deg) of $\text{Ca}_6\text{-A}$ Treated with Rb Vapor

	Crystal 1	Crystal 2
(Si, Al)-O(1)	1.632(9)	1.62(2)
(Si, Al)-O(2)	1.630(10)	1.62(4)
(Si, Al)-O(3)	1.670(7)	1.68(2)
Rb(1)-O(2)	3.34(2)	3.40(5)
Rb(1)-O(3)	3.60(2)	3.57(3)
Rb(2)-O(1)	3.321(4)	3.323(8)
Rb(2)-O(2)	2.865(9)	2.83(2)
Rb(3)-O(2)	3.42(1)	3.28(3)
Rb(3)-O(3)	2.85(2)	2.87(4)
Rb(4)-O(1)	3.2(3)	3.3(1)
Rb(4)-O(3)	3.2(2)	3.20(9)
Rb(1)-Rb(2)	5.132(2)	5.129(5)
Rb(1)-Rb(4)	4.4(2)	4.3(2)
Rb(2)-Rb(2)	5.552(5)	5.54(1)
Rb(2)-Rb(3)	3.49(1)	3.46(1)
Rb(3)-Rb(3)	4.49(1)	4.58(2)
	3.66(1)	3.74(3)
O(1)-(Si, Al)-O(2)	109.7(9)	116(2)
O(1)-(Si, Al)-O(3)	112.4(7)	109(1)
O(2)-(Si, Al)-O(3)	106.0(5)	103(2)
O(3)-(Si, Al)-O(3)	110.0(5)	116(1)
(Si, Al)-O(1)-(Si, Al)	144(2)	149(4)
(Si, Al)-O(2)-(Si, Al)	165.1(8)	174(2)
(Si, Al)-O(3)-(Si, Al)	143.9(8)	142(2)
O(3)-Rb(2)-O(3)	86.5(3)	88.0(7)
O(3)-Rb(3)-O(3)	87.1(2)	86.2(7)
Rb(2)-Rb(3)-Rb(3)	144.7(4)	144.7(6)

Numbers in parentheses are estimated standard deviations in the least significant digit given for the corresponding values.

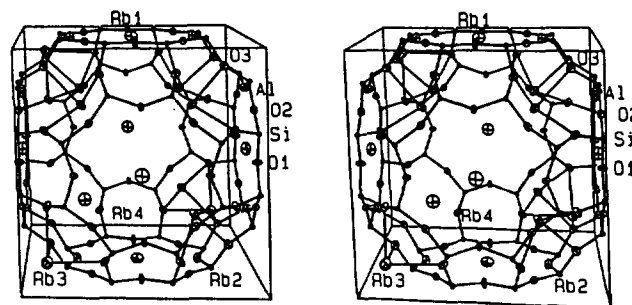


Figure 1. A stereoview of a large cavity of dehydrated Rb^+ -exchanged zeolite A exposed to excess $\text{Rb}(g)$. 3 Rb^+ ions at Rb(1), 6 Rb^+ ions at Rb(2), 3 Rb^+ ions at Rb(3), and 1 Rb^+ ion at Rb(4) are shown. Ellipsoids of 20% probability are used.

plane at O(3). In the sodalite unit, Rb(3) is *ca.* $2.86(4) \text{ \AA}$ from the O(3) of its 6-ring and *ca.* $1.75(1) \text{ \AA}$ from the (111) plane O(3) (see Tables 2 and 3).

In the large cavity, *ca.* 6 to 6 4/5 Rb^+ ions are found opposite the 6-rings at Rb(2) (see Table 1). In the sodalite unit, *ca.* 3 Rb^+ 's are found opposite the 6-rings at Rb(3). The sum

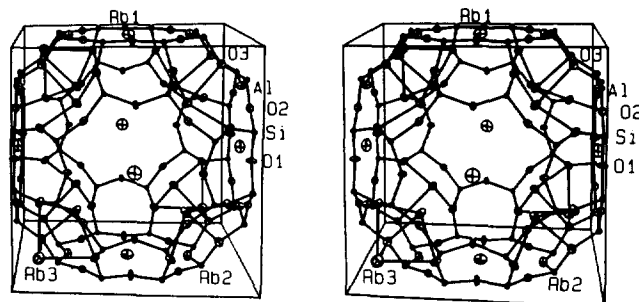


Figure 2. A stereoview of a large cavity of dehydrated Rb⁺-exchanged zeolite A exposed to excess Rb(g). 3 Rb⁺ ions at Rb(1), 8 Rb⁺ ions at Rb(2), and 3 Rb⁺ ions at Rb(3) are shown. Ellipsoids of 20% probability are used.

Table 3. Deviations of atoms (Å) from The (111) Plane at O(3) of Ca₆-A Treated with Rb Vapor

	Crystal 1	Crystal 2
O(2)	0.112(9)	0.078(21)
Rb(2)	1.754(3)	1.689(5)
Rb(3)	-1.727(9)	-1.767(12)
Rb(4)	3.174(152)	3.199(77)

A negative deviation indicates that the atom lies on the same side of the planes as the origin.

Table 4. Inferred Unit Cell Compositions for the Crystal 1 and Crystal 2

Positions of cations and atoms		Crystal 1		Crystal 2	
		80%	20%	60%	40%
8-ring	Rb(1)	3	3	3	3
6-ring	Rb(2)	6	6	6	8
	Rb(3)	3	3	3	3
Opposite 4-ring	Rb(4)	0	1	1	0

of the occupancies of Rb⁺ ions on the threefold axes at Rb(2) and Rb(3) are 8.97(13) for crystal 1 and 9.70(22) for crystal 2. This indicates that more than the usual limit of eight 6-ring cations per unit cell are found.

Rb⁺ ion at Rb(4) lies opposite the 4-ring, which bridges two 6-rings. This Rb⁺ ion is rather far from the framework oxygens (*ca.* 3.2(1) Å from O(1) and O(3)) probably because of repulsive interaction with the adjacent Rb⁺ ions.

The fractional occupancies observed at Rb(2), Rb(3) and Rb(4) are explained by proposing that 3 types of the unit cells exist in these crystals (see Table 4). About 20% of these unit cells in crystal 1 and about 60% in crystal 2 may have 6 ions at Rb(2), 3 ions at Rb(3), and 1 ion at Rb(4) (see Figure 1). The Rb⁺ ions may be arranged to avoid unreasonably close cation-cation contacts like that found in the previously reported Rb⁺-exchanged zeolite A.^{17,18} About 80% of unit cells in crystal 1 may have 6 ions at Rb(2) and 3 ions at Rb(3). About 40% of unit cells in crystal 2 may have 8 ions at Rb(2) and 3 ions at Rb(3) (see Table 4).

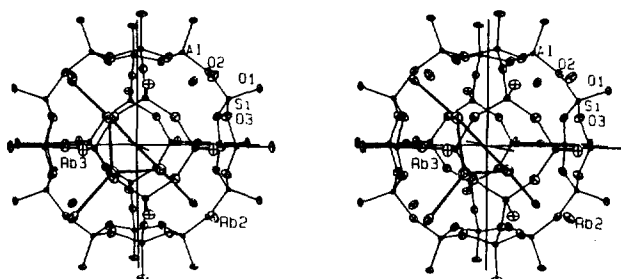


Figure 3. A stereoview of a sodalite cavities in dehydrated Rb⁺-exchanged zeolite A exposed to excess Rb(g). Each Rb(3) of the central triangle of the cluster interacts further with an Rb(2) to form the complete (Rb₆)⁴⁺ cluster. Ellipsoids of 20% probability are used.

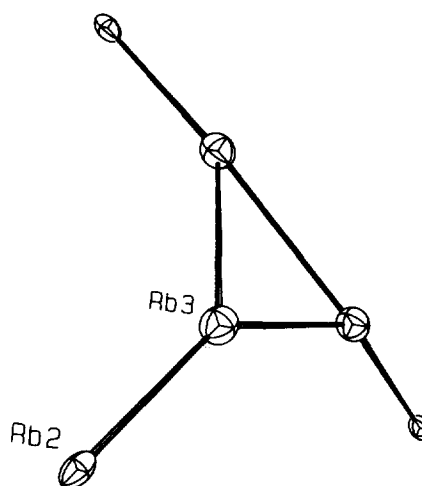


Figure 4. The (Rb₆)⁴⁺ cluster. It has 3*m* (C_{3v}) symmetry. Ellipsoids of 25% probability are used.

The unit cells of resulting crystals contain more Rb species than the approximately twelve Rb⁺ cations which are required to balance the anionic charge of the zeolite framework.

Three Rb(3)'s in sodalite unit must have Rb(3)-Rb(3) distances of 2.61 Å or 3.7 Å. The shorter distance is impossibly short, even less than the sum of the cationic radii of two Rb⁺ ions, 2.94 Å²⁰, and cannot be tolerated. To avoid it, the three Rb(3)'s must form an equilateral triangle with 3.7 Å distances (see Figure 3). These distances are still quite short as compared to the bond length in Rb metal, 4.95 Å²¹, for example, and this indicates that the electrons of the sorbed Rb atoms are at least partly delocalized over these three Rb(3) cations.

The eight Rb⁺ ions at Rb(2) are associated with sodalite units containing the Rb(3) triangle, to allow further electron delocalization. It follows that this sodalite unit has, associated with its 6-rings, eleven (3+8) Rb species, nine of which may be counted as Rb⁺ (to balance framework charge) and two as Rb⁰. The two electrons from these two Rb⁰'s per sodalite unit must be delocalized over the shortest Rb-Rb contacts in the structure, those among the three Rb(3)'s in the sodalite cavity and the three Rb(2)'s nearest to these Rb(3)'s, to give the (Rb₆)⁴⁺ cluster shown in Figures 3 and 4.

In the other structure, the Rb(3) triangle may be associ-

ated with two ions out of 6 Rb⁺ ions at Rb(2) because of repulsive interactions with Rb⁺ ion at Rb(4): two adjacent 6-ring sites of a Rb⁺ ion at Rb(4) should be vacant. Therefore, in this case, a cluster of (Rb₆)⁴⁺ may also be formed with much lower symmetry.

In this result, the reaction went to completion with 0.1 Torr of Rb(g) at 250°C for 2 hrs and 24 hrs, respectively, and all Ca²⁺ ions in dehydrated Ca₆-A were reduced and replaced by Rb⁺ ions. The Ca metal was not found within the zeolite but was seen coating the external surface of the zeolite crystals.

Acknowledgement. The present studies were supported in part by the Basic Research Institute Programs, Ministry of Education, 1992, project No. BSRI-92-306.

References

1. R. L. Firor and K. Seff, *J. Am. Chem. Soc.*, **99**, 1112 (1977).
2. J. J. Pluth and J. V. Smith, *J. Am. Chem. Soc.*, **105**, 2621 (1983).
3. N. H. Heo and K. Seff, *J. Phys. Chem.*, **109**, 7986 (1987).
4. N. H. Heo, C. Dejuspa, and K. Seff, *J. Am. Chem. Soc.*, **91**, 3943 (1987).
5. Handbook of Chemistry and Physics, 70th ed., Chemical Rubber Co., Cleveland, 1989/1990, p D157-158.
6. J. F. Charnell, *J. Cryst. Growth*, **8**, 192 (1971).
7. S. B. Jang, Y. W. Han, and Y. Kim, *J. Korean Chem. Soc.*, **35**, 630 (1991).
8. Reference 5, p D214-216.
9. K. Seff, *Acc. Chem. Res.*, **9**, 121 (1976).
10. K. Seff and M. D. Mellum, *J. Phys. Chem.*, **88**, 3560 (1984).
11. Principal computer programs used in this study were "Structure Determination Package Programs" written by B. A. Frenz and Y. Okaya. These programs were supplied by Enraf-Nonius, Netherlands, 1987.
12. International Tables for X-ray Crystallography, Kynoch, Birmingham, England, 1974, Vol. II, p. 132.
13. P. A. Doyle and P. S. Turner, *Acta Crystallogr., Sect. A, Cryst. Phys. Diffr., Theor. Gen. Crystallogr.*, **24**, 390 (1968).
14. Reference 12, Vol. IV, p. 73-87.
15. Reference 12, Vol. IV, p. 149-150.
16. C. S. Blackwell, J. J. Pluth, and J. V. Smith, *J. Phys. Chem.*, **89**, 4420 (1985).
17. S. H. Song, Y. Kim, and K. Seff, *J. Phys. Chem.*, **95**, 9919 (1991).
18. S. H. Song, U. S. Kim, Y. Kim, and K. Seff, *J. Phys. Chem.*, **96**, 0000 (1992) in press.
19. S. H. Song, Ph. D. Thesis, Pusan National University, (1991).
20. Reference 5, p F157.
21. Reference 5, p F189-190.

Conformation of Antifungal Agent Fluconazole

Seong Jun Han, Kee Long Kang[†], Sung Hee Lee[†], Uoo Tae Chung[†], and Young Kee Kang^{*}

*Department of Chemistry and [†]Department of Pharmacy, Chungbuk National University,
Chungbuk 360-763. Received October 27, 1992*

Conformational free energy calculations using an empirical potential function and a hydration shell model (program CONBIO) were carried out on antifungal agent fluconazole in the unhydrated and hydrated states. The initial geometry of fluconazole was obtained from two minimized fragments of it using a molecular mechanics MMPMI and followed by minimizing with a semiempirical AM1 method. In both states, the feasible conformations were obtained from the calculations of conformational energy, conformational entropy, and hydration free energy by varying all the torsion angles of the molecule. The intramolecular hydrogen bonds of isopropyl hydroxyl hydrogen and triazole nitrogens and the structural flexibility are of significant importance in stabilizing the conformations of fluconazole in both states. Hydration is proved to be one of the essential factors in stabilizing the overall conformation in aqueous solution. Two F atoms of phenyl ring are not identified as an essential key in determining the stable conformations and may be responsible for the interaction with the receptor of fluconazole.

Introduction

Fluconazole (UK-49,858, 2-(2,4-difluorophenyl)-1,3-bis(1*H*-1,2,4-triazol-1-yl)propan-2-ol) is a novel and water-soluble triazole antifungal agent, and has shown activity in several animal models of infection,¹ which is readily absorbed orally

and has a plasma half-life of 25 h, high blood levels, low levels of protein binding, and high urinary recovery.² In spite of the progress in the clinical evaluation against a range of fungal infections, any structural information of fluconazole is not available yet.

In the present study, the conformations of fluconazole in free space and aqueous solution were studied to determine its detailed structure and the hydration effect as a first step

^{*}Author to whom correspondence should be addressed.